Exp. Theo. NANOTECHNOLOGY 7 (2023) 67 - 77 https://doi.org/10.56053/7.2.67

Synthesis and characterization of polyethylene

X. Wang[1,*], *J. Whitaker*[2]

[1]Department of Materials Science and Engineering, University of Wisconsin-Madison, WI 53706, USA
[2]Center for Ultrafast Optical Science, University of Michigan, 2200 Bonisteel Blvd, Rm. 1006, Ann Arbor, MI 48109-2099 USA
*) Email: wangx@wisc.edu

A combined intumescent flame retardant expandable graphite (EG), with an initial expansion temperature of 155°C and expansion volume of 515 mL g-1, was successfully prepared based on a chemical intercalation method of material graphite under oxidation of KMnO4, intercalation of H2SO4 and Na4B2O7· 10H2O at the mass ratio C : KMnO4 : H2SO4 (98%) : Na4B2O7· 10H2O of 1.0 : 0.4 : 5.5 : 0.6 (H2SO4 diluted to a mass concentration of 80-wt. % before reaction), and characterized by expansion volume (EV), initial expansion temperature, X-ray diffraction (XRD). The flame retarding and thermal properties of LLDPE/EG and LLDPE/EG/APP composites (LLDPE-Linear low-density polyethylene; APP-ammonium polyphosphate) were investigated and characterized by limiting oxygen index (LOI), Fourier transform infrared spectroscopy (FTIR), thermal gravimetric (TG) and differential thermal analysis (DTA). The results showed that addition of EG (30-wt. %) increased the LOI of 70LLDPE/30EG composite to 28.4 %. Even more, the synergistic effect of 20% EG together with 10% APP improved the LOI of 70LLDPE/20EG/10APP composite to 30.5%. At the same time, temperatures corresponding to a 1% weight loss and a maximum weight loss rate increased at about 50°C and 2°C, respectively. The 70LLDPE/10APP/20EG composite exhibited higher flame retardancy even at a lower residual char than 70LLDPE/30EG specimen. The intercalated borate was more effectual in improving the flame retardancy than the direct additive of Na4B2O7· 10H2O.

Keywords: Graphite; Flame; Efficiency.

1. INTRODUCTION

Graphite is a crystalline compound with graphene plane's structure bonded by Van Der Waals force. Under oxidation, the graphite intercalating substance called expandable graphite could be prepared by chemical or electrochemical reaction inserting non- carbonaceous reactants into graphene planes [1-5]. Expandable graphite has been used as an intumescent type flame retardant for its good capability of halogen-free, non-dropping, low-smoke and low pollution potential [6,7]. When exposed to flame source, expandable graphite would form voluminous swollen multicellular char layers, which could protect materials from the heat of combustion, limit the diffusion of oxygen into the polymer, and reduce the production of smoke. Simultaneously, expandable graphite could absorb an enormous amount of heat during instant expansion, which could decrease the burning temperature. In addition, when graphite was oxidized by H2SO4 at high temperature, the releasing gases such as CO2, H2O could reduce the concentration of oxygen [8].

Linear low-density Polyethylene (LLDPE) is one of the most widely used polyolefin due to its balanced mechanical properties, chemical resistance, and ease of processing advantages. However, its inherent flammability has limited its applications in some fields where good flame retardancy is required. To solve this problem, many flame retardants have been applied in improving its flame retardancy, such as magnesium hydroxide [9], complex containing phosphorus, nitrogen [10], zinc borate [11], antimony trioxide [12], triazine containing flame retardant hyperbranched polyamines [13], and their synergistic effects [14,15]. It is well known that borate is one kind of important flame retardant with remarkable flame retardancy. Boric acid and hydrated borates hold low melting temperature, and they can absorb heat and lose water of crystallization. The water vapor caused by material decomposition may provide a dual function: it not only absorbs an enormous amount of heat, but also dilutes the concentration of the volatile oxidizable pyrolysis production in the flame zone, thereby enhanceing residual char formation. Furthermore, the residual boric oxide can form a glassy coating on the surface of polymer, limiting the transfer of heat and mass, as well as oxygen diffusion, and then retarding further combustion (Xue & Zeng, 1988). In the anti-flame test of LLDPE, the addition of zinc borate could improve the thermal stability and substantially enhance the residue carbon of APP-PER-LLDPE system [PER- pentaerythritol] [16]. Addition of the synthesized netlike nano-zinc borate 2ZnO· 3B2O3· 3.5H2O into polyethylene resulted in an increasing of residual char [17].

It is known that non-carbonaceous reactants can be inserted into graphene planes using chemical or electrochemical reaction, and the dilatability of expandable graphite can be affected by oxidant, intercalating agent and assistant intercalating agent. For examples, with graphite, KMnO4, HNO3 and HBrO3 used as reactant, expandable graphite with an initial expansion temperature of 130°C and expandable volume (EV) of 350 mL g-1 was prepared (Wang et al., 2009). Expandable graphite with an initial expansion temperature of 300°C and EV of 360 mL g-1 could be prepared using 50% H2SO4 and KMnO4 reacting for 30 min at 45°C [18], and its addition of 30-wt. % into ethylene vinyl acetate copolymer (EVA) could improve the limiting oxygen index (LOI) to 28.1%.

As a result, the purpose of this research was to prepare a combined intumescent flame retardant consisting of expandable graphite (EG) and borate in graphite intercalating reaction. To our

best knowledge, no study on this method and the EG flame retarding property for LLDPE has so far been reported in the literature. In intercalating reaction of material graphite, KMnO4, H2SO4 and sodium tetraborate (Na2B4O7· 10H2O) were used as oxidant [19,20], intercalating and assistant intercalating agent, respectively. The method of preparing EG fitting for flame retardancy of LLDPE was found, and its expansion property, structure characteristics were characterized by EV, initial expansion temperature and X-ray diffraction (XRD). The flame retardancy of LLDPE/EG and LLDPE/EG/APP composites were characterized by LOI. Fourier transform infrared spectroscopy (FTIR), thermal gravimetric (TG) and differential thermal analysis (DTA) were applied to illuminate thermal property and anti-flame mechanism.

2. EXPERIMENTAL

SX3-4-13 muffle furnace (Tientsin, China, precision of temperature ± 0.1%−0.4%°C); Y-4Q X-ray diffractometer (XRD) (Dandong, China); Muller (Jiangsu, China); Instrument of limiting oxygen index (LOI) (Chengde, China); TM3000 electron microscope (Japan); STA 449C thermal gravimetric (TG) and differential thermal analysis (DTA) (Germany) FTS-40 fourier transform infrared (FTIR) spectrograph (America Biorad) were used in this experiment.

Natural flake graphite was provided by Action Carbon CO. LTD, Baoding, China. Carbon content of flake graphite was 95 wt%, and an average flake size was 0.3 mm. Na2B4O7·10H2O, H2SO4 (98 wt%), KMnO4 were all analytical agents and bought from China. APP (I, n>50) was purchased from Sichuan, China. LLDPE 7540 was purchased from Daqing, China.

Reactants were weighed and mixed in the order of diluted H2SO4, Na2B4O7·10H2O, material graphite C and KMnO4 in a 250 mL beaker and stirred at a controlled temperature using a water bath. After maintaining for 40 min, the solid phase was washed with de-ionized water until pH of the waste water reached to 6.0−7.0. Solid product was dipped in water for 2 h, then filtrated and dried at 60-70oC for 6 h, and EG was obtained. The effects of various factors on dilatability of the EG were optimized through single factor tests including the dosages of KMnO4, H2SO4, Na2B4O7· 10H2O, H2SO4 concentration, reaction temperature and time. It was noticed that, KMnO4 dosage and H2SO4 concentration had important influence on intercalation of graphite. Too higher KMnO4 dosage and H2SO4 concentration would cause excessive oxygenation of material, which could lead to a decrease in EG granularity and dilatability. For examples: with H2SO4 diluted to 80-wt. % and dosage of KMnO4 increased from 0.4 g g-1 to 0.6 g g-1, EV of the EG decreased from 515 mL g-1 to 330 mL g-1, while, Finally, preparation conditions of EG with high dilatability and low expansion temperature were determined as follows: mass ratio of C: KMnO4: H2SO4(98%) : Na2B4O7· 10H2O was controlled as 1.0:0.4:5.5:0.6, H_2SO_4 was diluted to 80 wt%, and the reaction maintained for 40 min at 40°C, then EG with an initial expansion temperature of 155°C and maximum EV of 515 mL g-1 obtained. The expansion temperature curve of the EG was detected and shown in Figure 1. When temperature was among 600- 900°C, EV of EG was all above 400 mL g-1.

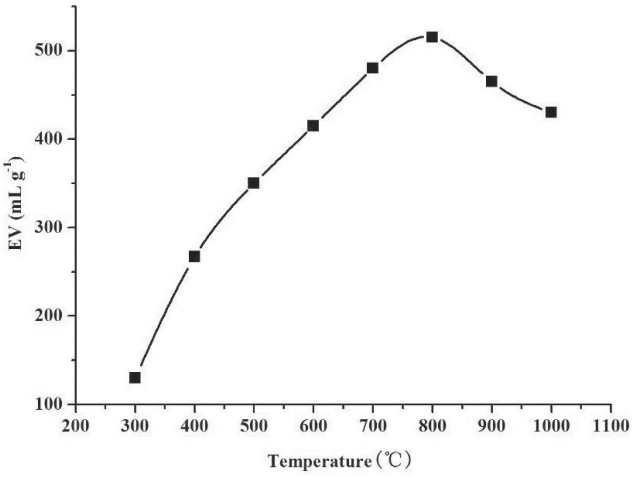

FIGURE 1 Expansion curve of EG.

XRD pattern was obtained under the operation condition of 40 kV, 30 mA, employing Ni-filtered Cu Kα radiation with 2θ ranging from 10° to 70°.

LOI is the minimum amount of oxygen in an oxygen-nitrogen mixture required to support combustion over 3 min. The LOI method is a simple, fast, and effective method of studying the flame retardancy of plastic materials. In this study, the flame retardancy of composites was measured by using the LOI values according to Standard of GB/T2406-1993 with oxygen index instrument.

Thermal analysis of the samples were carried out by TG with N2 flux of 25 mL min-1 and 10 mg of the sample was placed in porcelain crucible, then it was heated to 900°C at a heating rate of 10°C min-1. Changes of sample weight with increasing temperature were recorded. DTA was carried under N2 ambience with a flux of 25 Ml min-1. Residue morphology of flame retarding composites, formed after combustion, was investigated by electron microscope. The combusting residua were analyzed with FTIR spectroscopy with a resolution ratio of 2 cm-1 at the ranges of 400~4000 cm-1.

3. RESULTS AND DISCUSSION

XRD analysis results for material graphite, EG and EG1 were shown in Figure 2 (a), (b) and (c). As shown in (a), the two peaks with the interplanar crystal spacing of 3.34 Å and 1.67 Å corresponding to diffraction angle of 26.6°, 54.8° are the characteristic pattern of graphite. While, as shown in (b) and (c), the characteristic peaks of EG and EG1 shift to a small angle of 25.7° and 26.0°, respectively. Each corresponds to a bigger interplanar crystal spacing of 3.46 Å and 3.43 Å due to intercalation in graphene planes. More importantly, it is easily found that there is a new peak with the interplanar crystal spacing of 3.16 Å at 28.1° in (b). This can be explained that natural graphite is oxidized by oxidants and then exhibited positive charge (Avdeev et al., 1992a and 1992b; Zhu et al., 1998, Kuan et al., 2012). Due to the repulsion, the gap between graphite layers is extended, and intercalating reaction can proceed between graphite and intercalating agent. As shown in (b) and (c), EG holds bigger interplanar crystal

spacing than EG1 due to full intercalation reaction, so as to EG possess higher dilatability. As for the new diffraction presented at 28.1°, compared with standard XRD pattern, it should be sodium borate or sodium metaborate. For the known flame retardancy of borate and metaborate, it could be forecast that EG would present better flame retardancy than the contrast EG1.

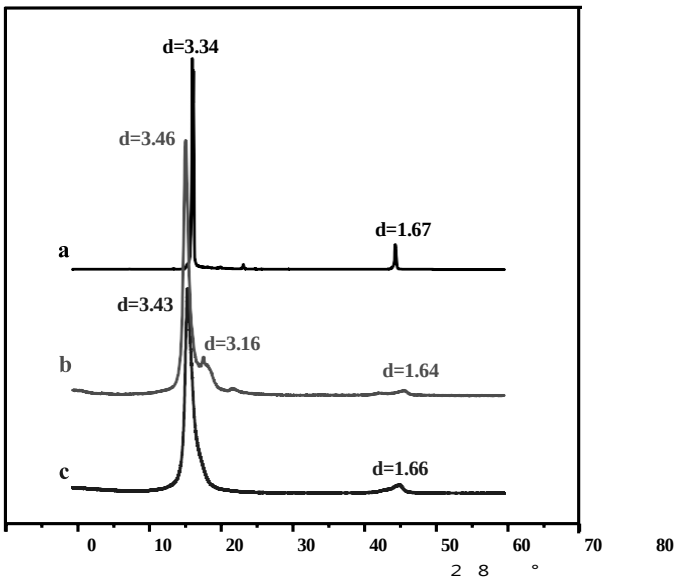

FIGURE 2 XRD analysis of material graphite and the prepared products (a) Material graphite; (b) EG; (c) EG_1

The processing temperature of LLDPE is lower than 140°C, so the prepared EG and EG1 can be used as retardant. Flame retardants were added into LLDPE according to the proportion listed in Table 1, and LOI of composites were detected. The results showed that addition of 30-wt. % EG improved LOI to 28.4%. But addition of the same amount of EG1 or commercial expandable graphite into LLDPE improved the LOI to 26% and 23% [21], respectively. These results indicated that the use of Na2B4O7· 10H2O in intercalating reaction of graphite improved flame retardancy of EG for LLDPE, and the prepared EG and EG1 were more effectual than commercial expandable graphite. When the ordinary APP (I) was added as retardant, the LOI was only 19.3% at a 30% dosage. But as for sample 4 of 70LLDPE/10APP/20EG, the LOI improved to 30.5% when 20% EG together with 10% APP (I) were used. The value was obviously higher than the calculated LOI of 25.3% according to the single EG and APP (I) percent and LOI. Therefore, it may be inferred that there is synergistic efficiency between EG and APP.

In order to judge the retardance validity, the flame retardant efficiency (EFF) and the synergistic efficiency (SE) [22] were calculated according to Equation (1) and (2), respectively.

$$EFF = \Delta LOI/FR(\%) \quad (1)$$

Where ΔLOI is the change in the LOI, and FR is the flame retardant content. The higher the EFF, the greater the efficiency of the flame retardant is.

$$SE=EFF1 / EFF2 \quad (2)$$

Where EFF1 is the flame retardant efficiency of the synergistic system, and EFF2 is the flame retardant efficiency of a single flame retardant. SE is used to evaluate the synergistic efficiency of two or more flame retardants.

It is known that an effective char layer can improve flame retardants performance. In order to further investigate the effect of EG, APP on the char formation of LLDPE/ EG and LLDPE /APP/EG composites, the morphologies of the specimens after the LOI tests were characterized by electron microscope and were shown in Figure 3, (a), (b) and (c). As can be seen, EG changes to "graphite worm" on the surface of LLDPE (a), and the swollen multicellular char forms a heat insulation layer. Figure 3 (b) shows the incision section of 70LLDPE/10APP/20EG composite, the residue incision section is continuous and compact due to the conglutination of APP decomposing products; this structure provides a shield that insulates the substrate from radiant heat, and avoids the direct contact between substrate and flame. As for the 70EVA/30EG composite as shown in Figure 3 (c), the incision section is discontinuous with some small holes, originating from blowing gases in redox reaction between residual H2SO4 and the graphite according to the reaction (3). Finally, discontinuity and low mechanical strength of the residue cause the LLDPE/EG system a decrease in flame retardancy [23,24].

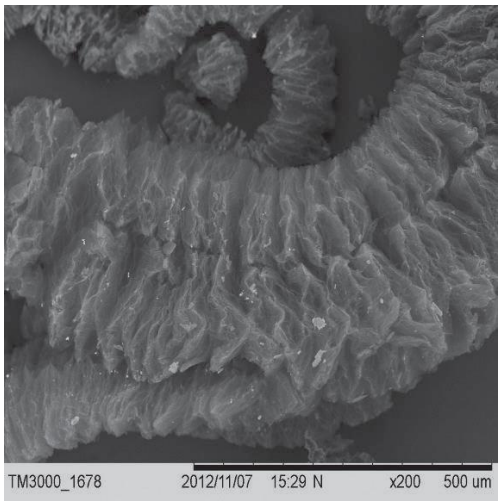

(a)

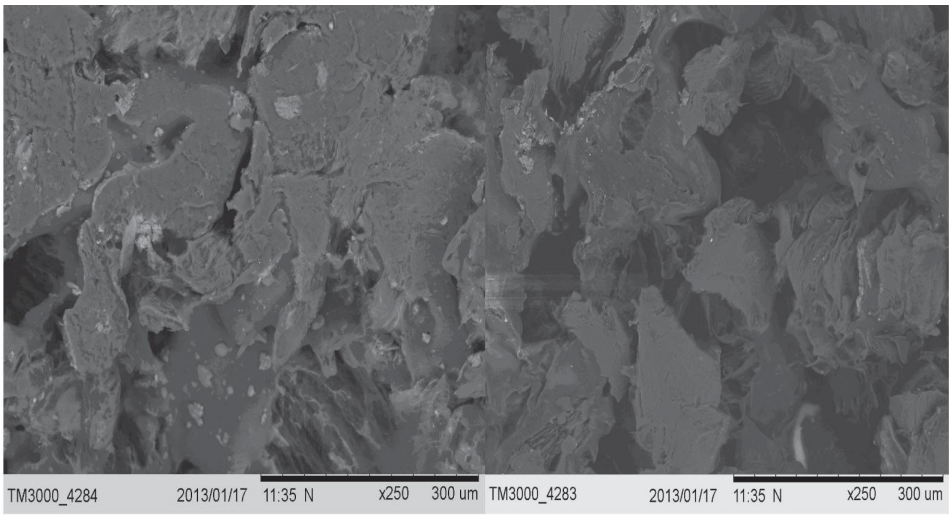

(b) (c)

FIGURE 3 SEM micrographs of carbonaceous chars (a)"worm like" expanded graphite (b) 70 LLDPE/10 APP/20EG (c) 70LLDPE/30EG.

To get the combustion residues and do the further analysis of FTIR, sample 4-6 adequately burned in Muffle furnace and maintained for 1 h at 800°C, then the residues and Na2B4O7· 10H2O agent were all analyzed with FTIR spectrograph, respectively. As shown in Figure 4, the appearance of specific absorption peak at 2924 cm-1 (corresponding to CH , CH groups) in 70LLDPE/10APP/20EG and 70 3 2 LLDPE/30EG proved that the addition of EG and APP was in favor of the formation of CH3, CH2 groups, improving thermal stability and retarding the further degradation of LLDPE. The peak strength of 70LLDPE/10APP/20EG was higher than that of 70LLDPE/30EG due to the synergism of EG and APP (I) [25]. Peaks at 1171 cm-1 and 1035 cm-1 in 70LLDPE/10APP/20EG are the characteristic peaks of P-O and P=O caused by APP (I) decomposition. As for the characteristic peaks of BO3, although they are not obvious due to the little inserting dosage, they still can be observed in 70LLDPE/10APP/20EG and 70LLDPE/30EG composites. Peaks at 700-400 cm-1 are normally the asymmetric stretching and bending of trigonal of BO3. Combining these results with XRD analysis of EG, it could be deduced that the possible form of B in EG was borate. For the known anti-flame property, the existence of the inserted borate could improve the flame retardancy of EG flame retardant.

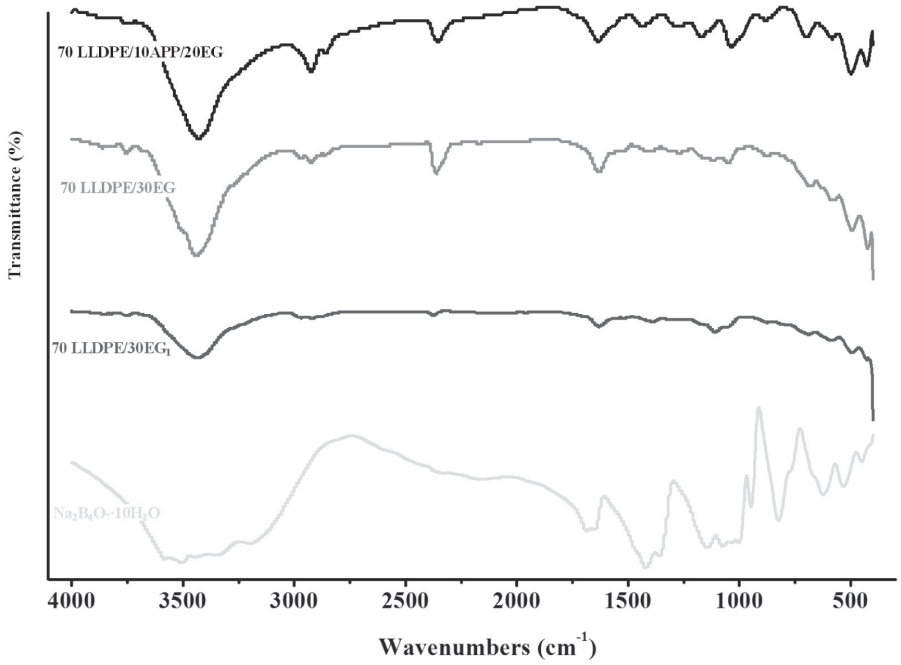

FIGURE 4 The FTIR for 70LLDPE/10APP/20EG, 70LLDPE/30EG, 70LLDPE/30EG$_1$ composites and $Na_2B_4O_7 \cdot 10H_2O$.

Figure 5 shows TG results of sample 4 of 70LLDPE/10APP/20EG composite and sample 5 of 70LLDPE/30EG specimen. The weight loss of these composites can be divided into two stages. The obvious weight loss occurs among 380-500°C. Among 100-380°C, weight loss is very slight, which is caused by the initial expansion of EG and decomposition APP (I). Temperature T1 corresponding to a 1% weight loss are 260°C for sample 4 and 207°C for sample 5, respectively. It can be seen that the addition of APP (I) leads to a higher T1 increased at about 50°C, which indicates sample 4 possesses higher thermal stability than sample 5. When temperature increases above 150°C, initial expansion of EG and decomposition of APP (I) occur, and the swollen EG worm can be felt together by the decomposing products of APP(I) and form into a compact multicellular carbonaceous char, retarding the transfer of heat and oxygen [22]. A 65%−70% weight loss occurs among the second stage of 380-500°C, caused by the full expansion of EG and combustion of LLDPE. For the well formation of multicellular carbonaceous char among 380- 500°C, further combustion is obviously retarded, and then the weight loss above 500°C is very slight. The final residual carbon is 21.09% for sample 4 and 28.68% for sample 5, respectively. For 70LLDPE/10APP/20EG composite, in spite of a lower residual carbon than 70LLDPE/30EG specimen, it exhibits a higher flame retardancy indicated by T1 and LOI. This is because the swollen EG worm can form a compacter carbonaceous char layer due to the conglutination of APP (I) decomposing products. Compared with residual carbon weight, the carbonaceous char compaction should play a more important role in improving thermal stability and flame retardancy.

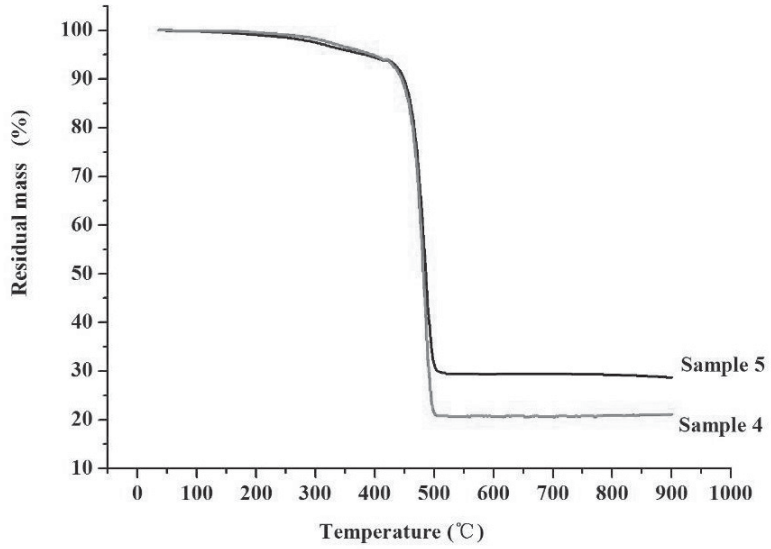

FIGURE 5 TG analysis of flame retarding LLDPE composites ample 4, 70LLDPE/10APP/20EG; sample 5, 70LLDPE/30EG.

5. CONCLUSIONS

We have developed a method that simplifies the process to generate lateral chromatic aberration correction factor and correct the lateral chromatic aberration. Since the predetermined chromatic aberration correction factor is applied to correct chromatic aberration prior to the image output, the method saves the hassle of post image analysis and calibration. By applying the proposed method into the case of small form factor and low-cost lens stack design, we can generate the lateral chromatic aberration correction factor during design stage. Although three element lens stacks were used for illustration here, we would like to emphasize that the method is not restricted solely to this optical systems – it is equally applicable in correcting different kinds of lens stack designs.

References

[1] A.Kumar, R. Vasantha, Exp. Theo. NANOTECHNOLOGY 4 (2020) 201
[2] Daniel Malacara, Handbook of Optical Design, CRC Press (2013)
[3] N. R. Farrar, A.H Smith, D.R. Busath, D. Taitano. Optical Cryotomography 40 (2000) 18
[4] J-S. Lim, Z-H. Jim, Exp. Theo. NANOTECHNOLOGY 4 (2020) 209
[5] Chao Chen and Bing Pan, Appl. Opt. 59 (2020) 6517
[6] C. Deke, E. P. Petrik, Exp. Theo. NANOTECHNOLOGY 4 (2020) 219
[7] BENJAMIN T. CECCHETTO, Correction of Chromatic Aberration from a Single Image Using Keypoints, Department of Computer Science, The University of British Columbia, 8, Feb (2020)
[8] Kim Ho Yeap and Kazuhiro Hirasawa, Introductory Chapter: Electromagnetism, InTechOpen, UK, Electromagnetic Fields and Waves, InTechOpen, UK, 15 May (2019)

[9] Warren J. Smith, Modern Optical Engineering, McGraw Hill, (2007)
[10] Joseph M. Geary. Introduction to lens design, Willmann-Dell, Inc, (2002)
[11] G. H. Smith. Practical Computer-Aided Lens Design, Willmann-Bell, Inc.c Richmond, VA, (1998)
[12] Rudolf Kingslake, Lens Design Fundamental, Academic Press, (2009)
[13] James P. McGuire Jr., Thomas G. Kuper, Approaching direct optimization of as-built lens performance, Proc. SPIE 8487, Novel Optical Systems Design and Optimization XV, 84870D, 19 October (2012)
[14] Jose Sasian, Lens Tolerancing, College of Optical Sciences, The University of Arizona. (2019)
[15] Kuang-Lung Huang, The tolerance analysis of wide-angle lens, Proceedings of SPIE - The International Society for Optical Engineering, February (2005)
[16] T. Philip, J. Maruc, K. Claire, Exp. Theo. NANOTECHNOLOGY 4 (2020) 231
[17] Soon-Wook Chung, Byoung-Kwang Kim, Woo-Jin Song, Removing chromatic aberration by digital image processing, Optical Engineering 49 (2010) 067002
[18] R. Willson and S. A. Shafer. Active lens control for high precision computer imaging, In Int'l Conf. on Robotics and Automation, pages 2063–2070, April (1991)
[19] Matsuoka, R., Asonuma, K., Takahashi, G., Danjo, T., Hirana, K., Evaluation of correction methods of chromatic aberration in digital camera images, In: ISPRS Photogrammetric image analysis. Volume I-3. (2012)
[20] Sanghui Han, John Kerekes , Shawn Higbee, Lawrence Siegel, Simulation techniques for image utility analysis, Proc. SPIE 10644, Algorithms and Technologies for Multispectral, Hyperspectral, and Ultraspectral Imagery XXIV, 106440P 8 May (2018)
[21] P. Wang, N. Mohammad, and R. Menon. Chromatic aberration-corrected diffractive lenses for ultra-broadband focusing, Scientific Reports 6 (2016) 2015
[22] Sing Bing Kang, Automatic Removal of Chromatic Aberration from a Single Image, IEEE Conference on Computer Vision and Pattern Recognition (2007)
[23] Victoria Rudakova, Pascal Monasse. Precise correction of lateral chromatic aberration in images, PSIVT, Oct 2013, Guanajuato, Mexico, (2013)
[24] Laikin, Milton. Lens design. CRC Press, (2018)
[25] Yue Zhong, Jun Chang, Weilin Chen, Shan Du, Zhongye Ji, Huilin Jiang & Jie Sui, Design and tolerance analysis of a large-diameter diffractive telescope, Journal of Modern Optics, 69 (2022) 566